




Detecting Disorders of Consciousness in Brain Injuries From EEG Connectivity Through Machine Learning

Fang Wang , Yu-Chu Tian , Senior Member, IEEE, Xueying Zhang , Member, IEEE, and Fengyun Hu

Abstract—Disorders of consciousness (DoC) happen frequently in various brain injuries. Their detection helps timely treatment for better survival outcomes of DoC patients. It is conventionally undertaken via clinical examinations, typically behavioural assessments. However, these neurological examinations consume significant resources of manpower and time, making continuous DoC monitoring practically infeasible. To address this issue, a computer-aided approach is proposed in this article for automated DoC detection through extracting knowledge from electroencephalogram (EEG) signals. It introduces a new connectivity measure: Power Spectral Density Difference (PSDD) incorporating with a recursive Cosine function (CPSDD). Then, the approach classifies brain-injured patients into DoC (i.e., positive) and wakefulness (i.e., negative) classes through an ensemble of support vector machines (EOSVM), which is a type of machine-learning methods. It is further applied to a dataset of 607 patients with brain injuries. Our classification results show that the EOSVM classifier with the new connectivity measure CPSDD has achieved the best classification performance among 12 connectivity measures. For a setting of 97% majority voting from all SVMs, the EOSVM has diagnosed, in high confidence, 35% of patients with the accuracy, sensitivity, and specificity of 98.21%, 100%, and 95.79%, respectively. Thus, the classifier EOSVM incorporating with the new connectivity measure CPSDD is a promising tool for automatic detection of DoC in brain injuries.

Index Terms—Machine learning, brain connectivity, disorders of consciousness (DoC), electroencephalogram (EEG).

Manuscript received May 29, 2020; revised August 30, 2020, September 20, 2020, and October 3, 2020; accepted October 11, 2020. This work was supported in part by the Department of Science and Technology of the Shanxi Provincial Government of China through the Key Research and Development Projects Scheme under Grant 201803D31045, the Australian Research Council (ARC) through the Linkage Project Scheme under Grant LP140100394, the Wu Jieping Medical Foundation of China under Grant 320675016129, and Research Project Supported by Shanxi Scholarship Council of China under Grant HGKY2019025. The associate editor coordinating the review of this manuscript and approving it for publication was Dr. Vesna Sesum-Cavic. (Corresponding authors: Yu-Chu Tian; Xueying Zhang; Fengyun Hu.)

Fang Wang is with the College of Information and Computer, Taiyuan University of Technology, Taiyuan 030606, China, and also with the School of Computer Science, Queensland University of Technology, GPO Box 2434, Brisbane, QLD 4001, Australia (e-mail: wang_fang_ty@163.com).

Yu-Chu Tian is with the School of Computer Science, Queensland University of Technology, Brisbane, QLD 4001, Australia (e-mail: y.tian@qut.edu.au).

Xueying Zhang is with the College of Information and Computer, Taiyuan University of Technology, Taiyuan 030606, China (e-mail: tyzhangxy@163.com).

Fengyun Hu is with the Department of Neurology, Shanxi Provincial People's Hospital affiliated with Shanxi Medical University, Taiyuan 030012, China (e-mail: fengyun71@163.com).

Digital Object Identifier 10.1109/TETCI.2020.3032662

I. INTRODUCTION

A DISORDER of consciousness (DoC) is a state where consciousness has been affected by damage to the brain. It has several sub-types including somnolence, stupor, light coma, middle coma, and deep coma. DoC happens frequently after acute brain injuries, such as haemorrhages, trauma, and stroke [1]. Accurate diagnosis of DoC is important to inform prognostic counselling and guide treatment decisions [2]. Patients with DoC frequently experience significant medical complications that can slow recovery and interfere with treatment interventions [3]. Traditionally, the level of consciousness is assessed via clinical observations and behavioural examinations, which carry a high test-retest and inter-examiner variability [4]. The awareness of the changes in the level of DoC largely relies on how long the interval to the next clinical examination is. Such clinical examinations consume significant manpower, time and other resources for both inpatients and outpatients [5].

Resting-state electroencephalography (EEG) monitoring is a potentially attractive tool to assist medical practitioners in a quick assessment of DoC after brain injuries. With portability and cost-effectiveness, it is usually used at the bedside of a patient [6]. In EEG investigations, EEG's brain connectivity, which refers to different interrelated aspects of brain organization, is a topic of much interest. It is normally divided into three different categories: anatomical or structural, functional, and effective brain connectivity [7]. In this paper, we focus on functional brain connectivity, which characterizes the statistical dependence between the signals stemming from two (or among many) distinct units within a nervous system (from single neurons to whole neural networks) [8]. Functional brain connectivity has been used to study brain networks associated with cognitive functions, spontaneous activities, and neurological disorders [9]–[11]. It is measured by the existence of any type of linear or nonlinear covariance between two neurophysiological signals [8].

Various types of EEG's functional connectivity measures have been investigated in neurological disorders. Three classic types of measures are linear connectivity measures, phase synchronization measures, and spectral measures:

- 1) Linear connectivity measures include the Pearson correlation coefficient (PCC) [12] and coherence (COH) [13]. They are most commonly studied in neuroscience.
- 2) The measures of phase synchronization between different brain regions appear promising in the analysis of the

spatial properties of EEG. For example, phase-locking value (PLV) is used to classify emotion recognition [12] and differentiate schizophrenia [14]. The phase lag index (PLI) is employed to detect changes in the connectivity in Alzheimers disease patients [15]. Weighted phase lag index (wPLI) in the high-gamma range is higher during wakefulness than during sleep [16].

- 3) Spectral analysis is the entry point for studying EEG dynamics. The power spectral density (PSD) shows an association with increasing age [17]. The brain symmetry index (BSI) shows a positive correlation with the NIH (National Institutes of Health) stroke scale [18].

Many studies have investigated the importance of EEG-derived connectivity in the diagnosis and prognosis of DoC. For example, it is revealed that patients with DoC have consistently decreased global mean connectivity over the whole brain in the alpha frequency band in comparison with healthy individuals [19]. It is also found that the alpha-band connectivity for patients in vegetative state (VS) is significantly lower than that in minimally conscious state (MCS), especially for the connectivity across distant sites [20], [21].

To achieve an automatic classification of DoC or wakefulness in brain injuries, we adopt machine learning techniques to learn knowledge from EEG data and then make predictions and inference. Machine learning has been employed in medical and health applications in various aspects. Examples include automatic detection of movement compensations in stroke patients [22], sleep stages analysis [23], cognitive failure detection [24], and prediction of breast and colon cancers [25]. All these efforts motivate us to use machine learning for DoC detection in brain injuries.

Our work in this paper makes two main contributions:

- 1) A new functional connectivity measure is introduced for distinguishing DoC and wakefulness in brain injuries. It is the difference between the power spectral density of two time-series (PSDD), which is incorporated with a recursive cosine function (CPSDD) for noise reduction.
- 2) An ensemble of support vector machines (EOSVM) is designed for the detection of DoC in brain injuries. Connectivity measures from each pair of electrodes are input to the classifier. The outputs of the classifier are classification results, i.e., the diagnosis of a patient to DoC (i.e., positive) or wakefulness (i.e., negative).

The paper is organized as follows: Abbreviations and notations are tabulated in Table I. Section II describes case selection and dataset. Section III introduces connectivity measures. Section IV presents our EOSVM design. In Section V, we compare connectivity measures and their regression results. Our EOSVM classification results are reported in Section VI. Finally, Section VII concludes the paper.

II. CASE SELECTION AND DATASET

The state of consciousness of a patient is determined by using a hierarchical battery of observation assessments. It is classified into six states: wakefulness, somnolence, stupor, light coma, middle coma, and deep coma. The procedure of consciousness assessment is given in our previous work [26].

TABLE I
ABBREVIATIONS AND NOTATIONS

COH, CCOH	COHerence, COH with recursive Cosine
DoC	Disorder(s) of consciousness
EEG	Electroencephalogram
EOSVM	Ensemble of SVM
ICOH, CICOH	Imaginary part of COH, ICHOH with recursive Cosine
PCC, CPCC	Pearson Correlation Coefficient, and PCC with recursive Cosine
PLI, CPLI	Phase Lag Index, and PLI with recursive Cosine
PLV, CPLV	Phase-Locking Value, and PLV with recursive Cosine
PSD	Power Spectral Density
PSDD, CPSDD	PSD difference, PSDD used with recursive Cosine
SD	Standard Deviation
SVM	Support Vector Machine
c_p, c_n	Positive and negative counts from n SVM outputs
F_n, F_p	False negatives, and false positives, respectively
$G_x(0), G_x(N)$	DCT coefficients
m, M	Integers used in DCT
N	Indicating N th DCT coefficient, or an integer number
n	The number of SVMs in EOSVM
R, R^2	Statistical measures
N_p, N_n	Positives and negatives in the entire dataset
R_F, R_T	Rates of false and true predictions in high confidence
R_H, R_L	Rates of predictions with high and low confidence
T_n, T_p	True negatives & true positives in high confidence range
$x(t), x_1(t), x_2(t)$	EEG signals after band pass filtering
$y(t)$	Signals output from recursive cosine
α	Voting threshold, $\alpha \in [0.5, 1]$

*Abbreviations and notations not frequently used are not listed here.

Participants in this study are inpatients admitted to the neurology department at Shanxi Provincial Peoples Hospital from June 2017 to December 2018. In this study, 607 subjects are selected in total. These subjects suffer from brain injuries including cerebral infarction, cerebral haemorrhage, intracranial infection, and epilepsy. Table II summarizes the demographics and clinical characteristics of these subjects. For all patients, clinical examinations with the assessments of consciousness including response to pain, arousal reaction, spontaneous acts, tendon reflex, light reflex and vital signs were performed immediately before EEG signals were recorded. In addition, all clinical assessments were performed by medical practitioners, who were blind to the subjects EEG connectivity measures. The exclusion criteria were as follows: (1) age < 18 years or (2) pregnant women. All data were collected as part of a prospective observational cohort study approved by the local institutional review board.

EEG is recorded using a digital video EEG bedside monitoring system (Solar 2000 N, Solar Electronic Technologies Co., Ltd, Beijing, China; sampling rate = 100 Hz). In the experiments, Ag/AgCl electrodes are positioned at FP1, FP2, C3, C4, O1, O2, T7, T8, A1, and A2 according to the international 10-20 system. They are placed in close contact with the surface of the skin and are routinely checked to keep impedance below 10k Ω . The reference/ground electrodes are A1 and A2.

EEG pre-processing is carried out offline in MATLAB (Mathworks, Natick, MA) using the EEGLAB (version 14.1.1b) toolbox. For each subject, ten minutes of EEG signals are selected for analysis in this study. The pre-processing procedure in this paper includes the following four steps: (a) Detecting bad EEG channels based on the statistics of neighbouring channels and subsequent distance weighted linear interpolation; (b) Re-referencing

TABLE II
DEMOGRAPHICS AND CLINICAL CHARACTERISTICS OF SUBJECTS USED IN OUR STUDY

Disease	Number of Subjects	Age Mean, SD	States of Consciousness (Females / Males)					
			Wakefulness	Somnolence	Stupor	Light Coma	Middle Coma	Deep Coma
Cerebral Infarction	201	65.28, 13.88	94 / 34	26 / 11	9 / 8	5 / 6	3 / 3	2 / 0
Cerebral Hemorrhage	43	65.81, 15.21	13 / 6	4 / 5	3 / 4	3 / 2	1 / 1	1 / 0
Epilepsy	46	50.98, 18.31	19 / 20	1 / 2	0 / 1	1 / 2	0 / 0	0 / 0
Intracranial Infection	47	41.17, 14.90	12 / 14	2 / 2	1 / 4	0 / 5	1 / 4	0 / 2
Others	270	54.98, 19.83	115 / 78	22 / 15	5 / 7	4 / 7	5 / 3	2 / 7
OVERALL	607	57.57, 18.63	253 / 152	55 / 35	18 / 24	13 / 22	10 / 11	5 / 9

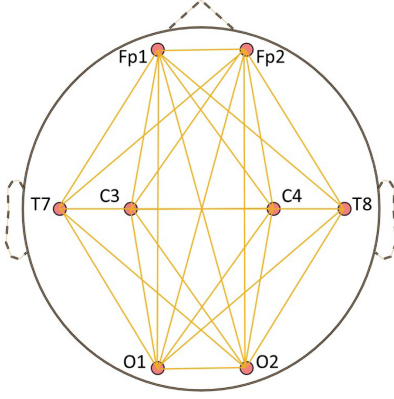


Fig. 1. Brain network.

each channel signal to an average reference; (c) High-pass filtering (0.5 Hz) and low-pass (40 Hz) filtering through a basic finite impulse response (FIR) filter; and (d) Detecting and removing artefacts through the automatic continuous rejection tool in EEGLAB with the following settings: frequency range 20–40 Hz, frequency threshold 10 dB, epoch segment length 0.5 s, the minimum number of contiguous epochs as 4, adding trails before and after 0.25 s, and also using Hanning window before computing FFT as a tick.

Additionally, in the third step (c) stated above, EEG recordings are filtered to obtain the signals of ten frequency bands: delta (1–4 Hz), theta (4–7 Hz), low alpha (8–10 Hz), high alpha (10–12 Hz), alpha (8–12 Hz), low beta (13–16 Hz), mid beta (17–20 Hz), high beta (21–29 Hz), beta (13–29 Hz), and gamma (30–40 Hz). Thus, connectivity measures are respectively extracted from these ten frequency bands.

III. EXTRACTION OF CONNECTIVITY MEASURES

A. Brain Network

The relationship between brain regions can be described as a brain network whose vertices and edges correspond to brain regions and their connections, respectively (Fig. 1). If the edges are weighted, they represent the strength of the connections with continuous values. This paper considers weighted edges in the brain network. Fig. 1 reveals 28 edges from eight electrodes: Fp1, Fp2, C3, C4, O1, O2, T7, and T8. We calculate 12 functional connectivity measures as the weights of the edges in the brain network in the following two sections. For each connectivity measure, 280 features are obtained from 28 channel pairs \times 10 frequency bands (the delta, theta, low alpha, high alpha,

alpha, low beta, mid beta, high beta, beta, and gamma) in our classification experiments.

B. Connectivity Between Two Electrodes

We consider six connectivity measures, in which two linear measures, two-phase synchronization measures, and two nonlinear measures are included. Linear measures are PCC and COH; phase synchronization measures are PLV and PLI; nonlinear measures are PSDD and ICOH (Imaginary part of COH). These six measures of each frequency band are extracted from EEG signals for every pair of electrodes.

As PSD is one of the most commonly used measures to describe the activation level of an EEG signal [12], we introduce PSDD to measure the power difference of different regions in the brain. PSDD of all the channel pairs in the brain can demonstrate the power difference distribution of the whole brain. Firstly, we compute the PSD of the EEG signal for each electrode by using Welch's method. Then, we compute the PSDD of x_1 and x_2 as follows:

$$PSDD = |PSD(x_1) - PSD(x_2)|, \quad (1)$$

where $PSD(\cdot)$ is the PSD of the input signal. It is found by using Welch's overlapped segment averaging estimator.

PCC and COH are classical linear measures. PCC [12] describes the linear relationship of two signals $x_1(t)$ and $x_2(t)$:

$$PCC = \frac{cov(x_1, x_2)}{\sigma_{x_1} \sigma_{x_2}}, \quad (2)$$

where $cov(\cdot)$ means covariance, and σ_{x_1} and σ_{x_2} are the standard deviations of x_1 and x_2 , respectively.

COH is a normalized linear measure of correlations between two signals within a certain frequency band [8]. It is sensitive to changes in power and also changes in phase relationships [27]. For two EEG channels $x_1(t)$ and $x_2(t)$, let $S_{x_1 x_2}(f)$ denote the cross power spectral density of two EEG channels $x_1(t)$ and $x_2(t)$. It is calculated by using Welch's averaged, modified periodogram method of spectral estimation. Also, let $S_{x_1 x_1}(f)$ and $S_{x_2 x_2}(f)$ denote the individual power spectral densities of $x_1(t)$ and $x_2(t)$, respectively. Then, COH between $x_1(t)$ and $x_2(t)$ is defined as:

$$COH = \frac{|S_{x_1 x_2}(f)|^2}{S_{x_1 x_1}(f) S_{x_2 x_2}(f)}. \quad (3)$$

Taking the imaginary part of COH, ICOH is defined as:

$$ICOH = \text{Imag}(COH). \quad (4)$$

PLV and PLI are phase synchronization measures, which refer to a situation when the phases of two coupled oscillators synchronize, even though their amplitudes may remain uncorrelated. PLV [27] estimates how the relative phase is distributed over the unit circle [14]. It takes the absolute average of phase differences over temporal windows:

$$PLV = \frac{1}{N} \left| \sum_{k=0}^{N-1} e^{i\Delta\phi(t_k)} \right|, \quad (5)$$

where $\Delta\phi$ represents the phase difference of a pair of electrodes, N is the number of samples of each signal, $x_1(t)$ and $x_2(t)$ (here, $\Delta\phi$ is calculated in the same way as our previous study [28]); i represents the imaginary unit; t_k represents the k th discrete time-step.

PLI [15] is considered more robust to the common source problem than PLV. This is because it discards phase distributions that center around $0 \bmod \pi$. PLI is defined as:

$$PLI = \frac{1}{N} \left| \sum_{k=0}^{N-1} \text{sign}(\Delta\phi(t_k)) \right|, \quad (6)$$

where $\text{sign}(\cdot)$ is the sign function, N is the number of samples from each signal, and t_k represents the k th discrete time-step.

C. New Connectivity Measure With Recursive Cosine Function

The connectivity measures discussed above are the commonly used ones so far. While they have their applications, they are not effective enough in assessing the state of consciousness in brain injuries. This is due to the fact that artefacts and noise contamination in EEG signals are often much larger than the genuine electrical activity of the brain, especially in EEG from brain injury patients. Also, these noises may share the same frequency band with signal components of interests. Therefore, it is difficult to remove all noises through normal denoising methods [29], [30].

For noise reduction and thus improved extraction of useful information from EEG, we propose to incorporate a recursive cosine function with connectivity measures. The recursive cosine function is similar to the first coefficient of the discrete cosine transform (DCT). Attempting to correct the noisy amplitude, DCT concentrates its energy only on the first few transform coefficients (and thus neglects all other coefficients) [31]. The recursive cosine function reduces the noise amplitude in a similar way as DCT. The influence of DCT and the recursive cosine function on EEG signal will be compared later in V-A.

For a data sequence $x(m), m = 0, 1, \dots, (M-1)$, let $G_x(N)$ denote the N th DCT coefficient, $N = 1, \dots, M-1$. Then, the DCT of $x(m)$ is defined as

$$\begin{cases} G_x(0) = \frac{\sqrt{2}}{M} \sum_{m=0}^{M-1} x(m) \\ G_x(N) = \frac{2}{M} \sum_{m=0}^{M-1} x(m) \cos \frac{(2m+1)N\pi}{2M} \end{cases} \quad (7)$$

In this paper, we calculate from EEG signals PSDD, PCC, COH, ICOH, PLV, and PLI as the first group of connectivity

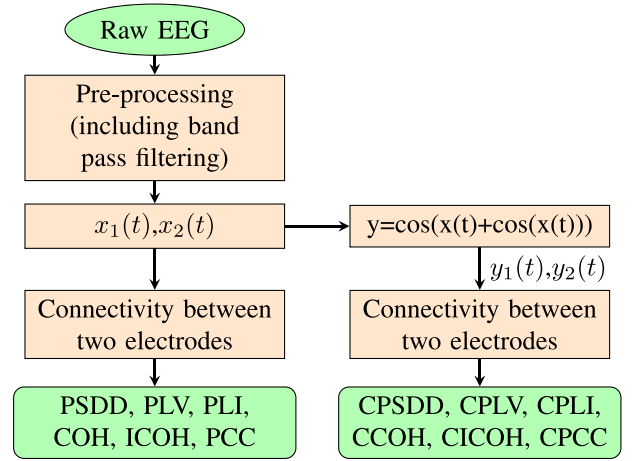


Fig. 2. The calculation of connectivity measures incorporating with the recursive cosine function in EEG pre-processing.

measures. These measures are also calculated incorporating with a recursive cosine function:

$$y(t) = \cos(x(t) + \cos(x(t))), \quad (8)$$

where $x(t)$ is a pre-processed form of an EEG signal from one electrode. This gives improved measures CPSDD, CPCC, CCOH, CICOH, CPLV, and CPLI, respectively, which form the second group of connectivity measures. The process of calculating connectivity measures is shown in Fig. 2.

D. Comparisons of the Two Groups of Connectivity Measures

In clinical examinations, the states of consciousness of patients are labelled as six states: wakefulness, somnolence, stupor, light coma, middle coma, and deep coma as mentioned in II. For convenience, we number the six states from 1 to 6, respectively. The bigger the numerical value of the level is, the worse the state of consciousness is.

With this numbering system, multiple linear regression models are used to test the correlation of the level of consciousness with the two groups of connectivity measures. The results of multiple linear regression models provide information on which connectivity measures are more effective than others in assessing the states of consciousness in brain injuries. Our experimental results will be presented later in Section V-B.

IV. ENSEMBLE OF SUPPORT VECTOR MACHINES

Datasets from the real world are generally imbalanced. EEG signals from the neurology department of a hospital normally consist of much more wakefulness (negative ‘-’) samples than DoC (positive ‘+’) ones. A common problem in dealing with imbalanced datasets is that the trained classifier is biased to the majority class. As a result, it is more likely to predict a sample as the majority class, which is the wakefulness (-) class in this study.

To address this classification problem, we design an EOSVM consisting of multiple support vector machine (SVM) classifiers. Each of the SVMs [32] is a binary classifier for classification of

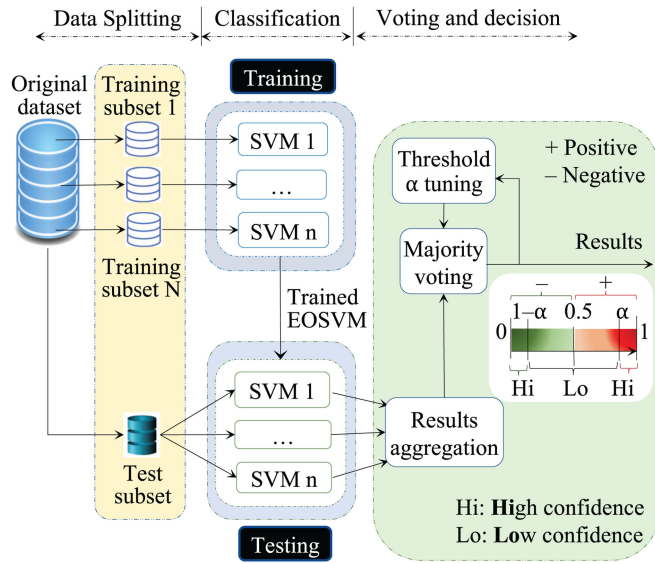


Fig. 3. The framework of the proposed EOSVM with n SVMs, each of which is a binary classifier.

a subject to either DoC (+) class or wakefulness (−) class. The number of SVMs in the EOSVM classifier, n , should be adjusted according to the distribution of the original dataset. Normally, the more heavily imbalanced the dataset is, the more SVMs should be used in the EOSVM classifier. In the experiments of this study, 100 SVMs are embedded into the EOSVM classifier. They show better performance in classification than other numbers of SVMs for the scenarios investigated in this study. Our tests of 10, 20, 30, 50 and 150 SVMs have given poorer classification performance.

The framework of our EOSVM is shown in Fig. 3 with a training phase and a testing phase. In the training phase, EOSVM is trained first from training data. Then, it is tested by using test dataset in the testing phase. The whole process of training and testing is performed in three steps: data splitting for training and testing, classification in training and testing, and voting for final results in testing. These three steps are described below in more detail.

A. Data Splitting for Training and Testing

Training the n SVMs independently in our EOSVM requires n sub-datasets. An additional sub-dataset is also required for EOSVM testing. Each of these training and testing sub-datasets is constructed from a subset of the original dataset. As shown previously in Table II, the 607 subjects in our original dataset include 202 DoC (+) subjects and 405 wakefulness (−) subjects. They are imbalanced in nature. There are different ways to deal with imbalanced data for classification. In this paper, we construct balanced sub-datasets from the original, imbalanced dataset shown in Table II. Fig. 4 illustrates the process of data splitting for training and testing subsets. It is explained below in detail.

The testing subset is constructed as follows: 1) randomly select 20% DoC subjects (40) from the 202 DoC subjects; 2)

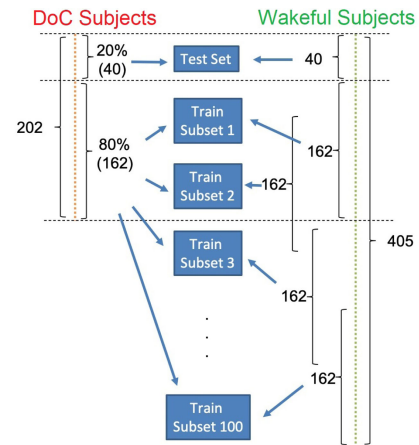


Fig. 4. Data splitting for our EOSVM with $n = 100$ SVMs.

randomly pick up the same number of wakefulness subjects (40); 3) mix up these 40 DoC subjects and 40 wakefulness subjects to form a balanced testing dataset. Thus, the testing dataset is composed of 80 subjects altogether.

The remaining subjects that have not been selected in the above testing dataset construction form our training dataset. They include 162 DoC subjects and 365 wakefulness subjects. They are used to construct n balanced training sub-datasets through the following process: 1) initialize n empty training subsets corresponding to n SVM classifiers; 2) place all 162 DoC subjects into each of the n training subsets; and 3) for each of n training subsets, if it has not been placed wakefulness subjects, add into it the same number (162) of wakefulness subjects from the 365 wakefulness subjects in the training dataset subject to the following two constraints:

- The selected 162 wakefulness subjects in building a new training subset are not all the same as those in the training subsets that have already been built; and
- All the 365 wakefulness subjects are placed into the n training subsets.

Thus, each of the training subsets consists of 324 subjects altogether (162 DoC subjects and 162 wakefulness subjects).

B. Classification in Training and Testing

As shown in Fig. 3, in the training phase of our EOSVM, each of the n SVM classifiers is trained on a different training subset for binary classification of each subject to either DoC (+) or wakefulness (−) class. The Gaussian kernel function is employed to train each SVM. Each of the SVMs automatically tunes the capacity of the classification function by maximizing the margin between training samples and class boundary. Hyper-parameters are also obtained after the process of the margin maximization operation.

In the testing phase of our EOSVM, the EOSVM trained above is fed with the test sub-dataset. For each data sample in the test subset, each of the SVMs gives a classification result of either DoC (+) or wakefulness (−). This means that for each data sample, n classification results will be obtained from the n SVMs. They will need further processing.

C. Voting and Decision Making in Testing

For each data sample in the test subset, the n binary classification results from the n SVMs may be the same or different ($n = 100$ in our case). Thus, they are aggregated to give a positive count c_p (e.g., 90) and a negative count c_n (e.g., 10), which sum up to n , i.e.,

$$c_p + c_n = n. \quad (9)$$

This process is shown in Fig. 3.

Then, the aggregated results are fused for a final classification result through a majority voting. In standard majority voting [25], the class value (+ or – in our case) with the most votes from the n SVM classification results is determined as the final classification result. For binary classification, the majority voting means that a sample data is classified into either Positive (DoC) class if $c_p > c_n$, or Negative (wakefulness) class otherwise.

However, a simple criterion of $c_p > c_n$ does not always give a clinically reliable result. This is because in clinical practice a false diagnosis is risky, which may result in serious consequences. If the values of c_p and c_p are similar, e.g., 51 versus 49, we only have low clinical confidence for the classification result of positive (DoC) class. If $c_p \gg c_n$ or $c_p \ll c_n$, the final classification result is more clinically reliable. Therefore, a voting threshold of $\alpha \in [0.5, 1]$ is defined to differentiate the final classification results with high and low clinical confidence. It is a decision variable in the decision-making step of the EOSVM testing phase as shown in Fig. 3. The threshold α is tuned for clinically reliable classification performance. Then, as shown in Fig 3, we have

The final classification result

$$= \begin{cases} \text{'+' with high confidence,} & \text{if } c_p/n \in (\alpha, 1]; \\ \text{'+' with low confidence,} & \text{if } c_p/n \in (0.5, \alpha]; \\ \text{'-' with low confidence,} & \text{if } c_p/n \in [1 - \alpha, 0.5]; \\ \text{'-' with high confidence,} & \text{if } c_p/n \in [0, 1 - \alpha). \end{cases} \quad (10)$$

The standard simple majority voting means $\alpha = 0.5$. A majority voting with $\alpha > 0.5$ is known as supermajority voting.

In our study, we have tested different settings of the majority-voting threshold of α in its full range from 50% to 100%. Then, a suitable threshold is chosen for the best classification results.

D. Performance Metrics for Classification

Depending on specific application domains or scenarios, various performance metrics can be used to evaluate the performance of classification and prediction. They are mostly derived from different combinations of four basic numbers: True Positives T_p , True Negatives T_n , False Positives F_p , and False Negatives F_n :

- T_p : the positives (DoC) identified correctly as positives;
- T_n : the negatives (wakefulness) identified correctly as negatives;
- F_p : the negatives (wakefulness) diagnosed incorrectly as positives (DoC); and
- F_n : the positives (DoC) diagnosed incorrectly as negatives (wakefulness).

Also, let N_p and N_n denote the total numbers of real Positives and Negatives, respectively, in the entire test dataset. If we consider both high- and low-confidence results in Eq. (10), then $N_p = T_p + F_n$ and $N_n = T_n + F_p$. However, if we focus only on the high-confidence results in Eq. (10), the sum of T_p and F_n in the high-confidence range may be less than N_p . This is because some positives may be classified into the low-confidence range. Similarly, the sum of T_n and F_p in the high-confidence range may be less than N_n .

Focusing on the high-confidence range in Eq. (10) from the entire test dataset, we use two groups of metrics to evaluate the performance of our EOSVM classifier. The first group is commonly used in classifications for statistical analysis, while the second group is used for evaluating classification results with high confidence characterized in Eq. (10).

1) *The First Group of Metrics*: This includes Accuracy, Sensitivity, and Specificity. These metrics are commonly used to evaluate the performance of classifications in machine learning. The Accuracy characterizes how accurately the total number of data samples in the high-confidence range are classified as True Positives (DoC) and True Negatives (wakefulness). The Sensitivity measures the ability of a test to detect True Positives (DoC). The Specificity quantifies the ability of a test to detect True Negatives (wakefulness).

$$Accuracy = \frac{T_p + T_n}{T_p + T_n + F_p + F_n}, \quad (11)$$

$$Sensitivity = \frac{T_p}{T_p + F_n}, \quad (12)$$

$$Specificity = \frac{T_n}{T_n + F_p}. \quad (13)$$

2) *The Second Group of Metrics*: This includes Rate of Predictions with high confidence (R_H), Rate of Predictions with low confidence (R_L), Rate of True Predictions in the high confidence range (R_T), and Rate of False Predictions in the high confidence range (R_F).

The metric R_H quantifies the ratio of the subjects in the high-confidence range to all subjects in the entire test dataset for a given majority voting threshold α , i.e.,

$$R_H = \frac{T_p + T_n + F_p + F_n}{N_p + N_n} \quad (14)$$

A higher value of R_H implies that more subjects in the entire test dataset will be classified with high confidence.

Similarly, R_L measures the ratio of the subjects in the low-confidence range to all subjects in the entire test dataset, i.e.,

$$R_L = \frac{(N_p - T_p - F_n) + (N_n - T_n - F_p)}{N_p + N_n} = 1 - R_H \quad (15)$$

For a more intuitive view of the performance of the classifier, two additional metrics R_T and R_F are introduced:

$$R_T = Accuracy \times R_H = \frac{T_p + T_n}{N_p + N_n} \quad (16)$$

$$R_F = (1 - Accuracy) \times R_H = \frac{F_p + F_n}{N_p + N_n} \quad (17)$$

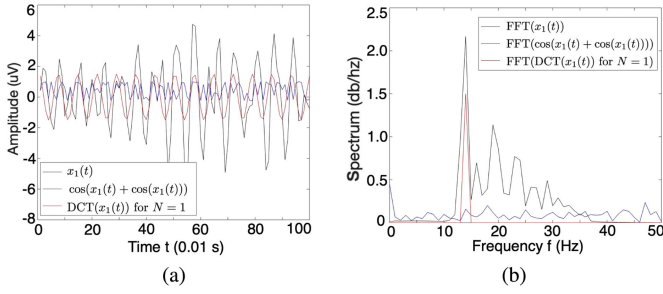


Fig. 5. The use of DCT and recursive cosine function in the processing of EEG signals. The $x_1(t)$ signal is a pre-processed EEG signal by using band pass filtering.

TABLE III
RESULTS OF REGRESSION

Model	Connectivity measure	Statistical Measures		Std. Err. of Estimation
		R	R^2	
1	PSDD	0.650	0.423	1.210
2	CPSDD	0.739	0.546 ↑	1.193
3	PLV	0.742	0.550	1.188
4	CPLV	0.777	0.603 ↑	1.115
5	PCC	0.755	0.571	1.159
6	CPCC	0.763	0.582 ↑	1.145
7	COH	0.773	0.597	1.124
8	CCOH	0.748	0.559 ↓	1.176
9	ICOH	0.750	0.563	1.171
10	CICOH	0.752	0.565 ↑	1.168
11	PLI	0.774	0.599	1.121
12	CPLI	0.687	0.472 ↓	1.287

R_T and R_F capture the ratios of True and False Predictions, respectively, in the high-confidence range indicated in Eq. (10) to all subjects in the entire test dataset. It follows that

$$R_T + R_F = R_H \quad (18)$$

V. RESULTS ON CONNECTIVITY MEASURES

A. Recursive Cosine Function and Discrete Cosine Transform

We evaluate the influence of the recursive cosine function $\cos(x_1(t) + \cos(x_1(t)))$, and DCT($x_1(t)$) with $N = 1$ (here N refers to the N th DCT coefficient) on EEG signal $x_1(t)$ from brain injuries. The evaluation results are shown in Fig. 5(a), where the $x_1(t)$ signal is not the original EEG signal but a pre-processed one by using band pass filtering. The corresponding spectrum of the EEG signal with the filtering function is depicted in Fig. 5(b).

It is seen from Fig. 5(a) that the phase patterns after using recursive cosine pre-processing and DCT pre-processing look similar. However, it is observed from Fig. 5(b) that $\cos(x_1(t) + \cos(x_1(t)))$ has better performance in removing the effects of amplitude than DCT does with $N = 1$ for $x_1(t)$.

B. Multiple Linear Regression

Multiple linear regression models are used to test the correlation of the level of consciousness with the 12 connectivity measures. They are summarized in Table III. For each of the 12 models, the inputs are 1) the level of consciousness (as a dependent variable) that goes from 1 to 6, and 2) the 280

features (as independent variables) from each of the connectivity measures. The outputs of each model are: 1) the goodness of fit of the models, and 2) the statistical significance (F-test) of the estimated parameters.

In Table III, statistical measures R and R^2 are used to check the goodness of fit of the models. Std. Err. of Estimation is the standard error of the estimated value. The determination coefficient (R^2) refers to how close the observed samples are around the regression curve. It is the main measure to assess the goodness of fit of each model here.

Comparing the R^2 values in Table III, we have observed that four of the second group of connectivity measures (CPSDD, CPCC, CICOH, and CPLV) have higher R^2 values than the corresponding ones in the first group of connectivity measures (PSDD, PCC, ICOH, and PLV). This means that incorporating the recursive cosine function with these four connectivity measures does improve the effectiveness of prediction on the states of consciousness in brain injuries.

VI. RESULTS AND DISCUSSIONS ON CLASSIFICATION

This study considers classifying a subject into one of two classes: the wakefulness subjects as Negative (−) class (class 1), and DoC as Positive class (class 2). In the ground truth data shown in Table II, the numbers of wakefulness and DoC subjects are 405 and 202, respectively.

In our classification, 12 connectivity measures from the two groups discussed previously are input as features into the EOSVM classifier. The first group includes PSDD, PCC, COH, ICOH, PLV, and PLI; while the second includes CPSDD, CPCC, CCOH, CICOH, CPLV, and CPLI. The states of consciousness (DoC or wakefulness) are also inputted to the EOSVM classifier as labels.

For each of the connectivity measures, a matrix of 280 features \times 607 subjects is input as features to the classifier. For each subject, ten minutes of EEG signals are selected. The connectivity measures from each channel pairs and each frequency are averaged over the ten minutes of time series.

A. Classification From Classical Classifiers

First of all, we use six well-developed classifiers to classify the subjects in our dataset to find out which classifiers are more effective than others. The classifiers we have tested include a fitted binary classification Tree, SVM, Linear Discrimination Analysis (LDA), AdaBoost, K-Nearest Neighbor (KNN), and Bagging. The method “Bagging” is an ensemble of decision trees. It implements the random forest algorithm in this work. The connectivity measure CPLV is input as a feature into the classifications. To achieve stable results, each classifier is executed 30 times.

Fig. 6(a) shows the performance of accuracy, sensitivity, and specificity of these six classifiers on the original dataset. It is seen from these box plots that the accuracy is about 70% for all these classifiers. The Tree classifier has the specificity performance lower than 80%, while all other classifiers have a specificity of around 90%, which is reasonably good. However, the results of sensitivity from all these classifiers are under 50%, which are poor for a clinically confident diagnosis decision. Thus, the

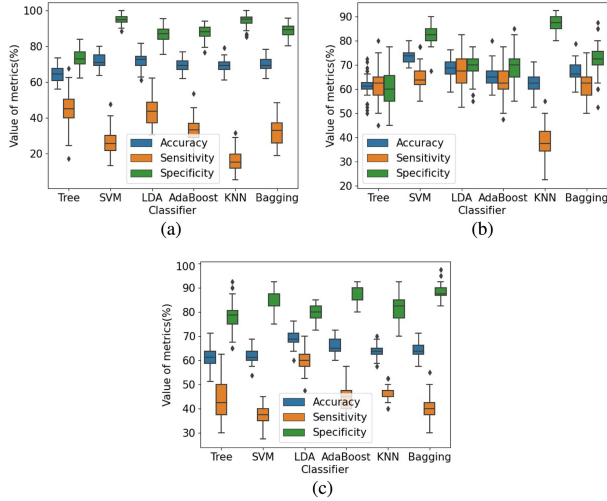


Fig. 6. Classification from six different classifiers: fitted binary classification Tree, SVM, LDA, AdaBoost, KNN, and Bagging implementing random forest.

classification results from these classifiers on the original dataset are not acceptable.

For classifications on an imbalanced dataset, re-sampling is a commonly used method for the improvement of classification performance. Therefore, we employ random under- and over-sampling methods to construct balanced datasets from the original dataset. Then, the classifications are undertaken on the balanced datasets. The results are depicted in Fig. 6(b) on the random under-sampling dataset and Fig. 6(c) on the random over-sampling dataset.

It is observed from Fig. 6(b) that the sensitivity of all classifiers except KNN has increased to over 60%. The sensitivity values from classifiers LDA and SVM are the two highest (around 69% and 65%, respectively). Between LDA and SVM, SVM shows higher accuracy and specificity (around 75% and 82%, respectively) than LDA (about 70% and 71%, respectively). Therefore, from the under-sampling dataset, SVM outperforms all other classifiers.

For the random over-sampling dataset, it is seen from Fig. 6(c) that the sensitivity of all classifiers except LDA remains under 50%. For LDA, the sensitivity is only increased to about 60%, which is not as good as LDA's 69% and SVM's 65%, respectively, on the under-sampling dataset shown in Fig. 6(b).

In summary, among the classifiers we have tested, SVM behaves the best from the random under-sampling dataset. This has motivated us to design our SVM-based EOSVM classifier with more than one SVM for further improvement of the classification performance. The process of data splitting for constructing balanced training and testing datasets has been presented previously in Fig. 4.

B. Classification From EOSVM

Following the process shown in Fig. 4, we have constructed $n = 100$ training subsets each with 324 subjects. We have also constructed an additional testing subset with 80 subjects. Inputting the testing subset into the trained EOSVM, we get $n = 100$ classification results from the $n = 100$ SVMs for each of the 80 subjects in the subset. These results are aggregated

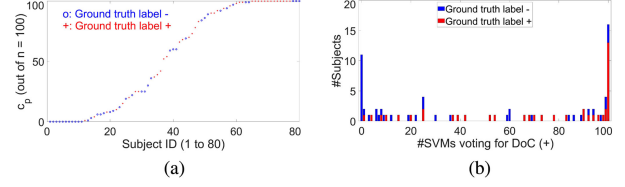


Fig. 7. Aggregated classification results from $n = 100$ SVMs for all 80 subjects in the testing dataset. In the plot of c_p , all subjects are sorted in an ascending order of their c_p values.

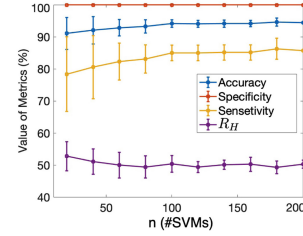


Fig. 8. Classification performance from different numbers of SVMs in EOSVM with the connectivity measure CSPDD and majority voting threshold $\alpha = 0.9$.

for further fusion, as shown in Fig. 3. The aggregated SVM classification results for all the 80 subjects are shown in Fig. 7.

From these aggregated results of SVM outputs, a standard simple majority voting will classify a subject with $c_p > n/2 = 50$ to the DoC (+) class and a subject with $c_p \leq n/2 = 50$ to the wakefulness (−) class. It is seen from Fig. 7(a) that the first few subjects with c_p close to 0 and the last few subjects with c_p close to $n = 100$. Thus, it is clinically confident to diagnose these subjects to either DoC (+) or wakefulness (−) though there would still be a few false positives and false negatives as shown in both Fig. 7(a) and Fig. 7(b).

However, the aggregated results are shown in Fig. 7(a) and Fig. 7(b) indicate that there are some subjects with c_p/n close to 50%, implying that the numbers of SVM outputs voting for DoC (+) and wakefulness (−) close to half-half. The above-mentioned simple majority voting will lead to high numbers of False Positives (F_p) and False Negatives (F_n). This motivates the use of the majority-voting threshold α defined in Eq. (10) as a decision variable to tune the performance of the final EOSVM classifications.

In our experiments, we have tested different settings of α in a wide range. From our experiments, the classification performance declines rapidly when α decreases to below 90%. Therefore, we focus on presenting our experimental results for the settings of α in the range of 90% to 100%.

1) *Results From Different Numbers of SVMs*: We have tested the classification performance of EOSVM under different number of SVMs from $n = 10$ to $n = 200$. The connectivity measure used in these tests is CPSDD. The majority voting threshold is fixed at $\alpha = 0.9$. The classification performance of Accuracy, Specificity, Sensitivity, and R_H is summarized in Fig. 8 under different numbers of SVMs.

The first observation from Fig. 8 is that the accuracy and sensitivity are higher when more than one SVM is employed (Fig. 6(b)). Also, it is seen from Fig. 8 that the accuracy and

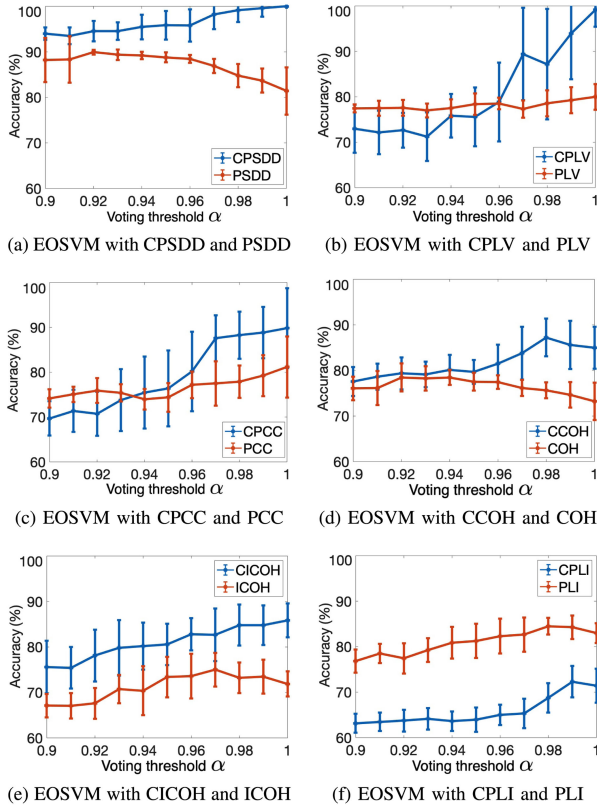


Fig. 9. The accuracy of EOSVM classifications from two groups of connectivity measures (The first group: PSDD, PCC, COH, ICOH, PLV, and LI; and the second group: CPSDD, CPCC, CCOH, CICOH, CPLV, and CPLI).

sensitivity rise when n increases from 10 to 100, and then remains stable when n further increases. The specificity remains the same at 100% for all settings of n in the range of 10 to 200. R_H , the rate of predictions in the high-confidence range indicated in Eq. (14), gradually drops when n increases from 10 to 80, and then shows slight fluctuations beyond $n = 100$. Considering these classification results, we choose 100 SVMs (i.e., $n = 100$) in our EOSVM configuration. This configuration will be used in the following experiments.

2) *Classification From the Two Groups of Connectivity Measures:* The accuracy of EOSVM classifications from two groups of connectivity measures is shown in Fig. 9. It is presented with respect to different settings of the voting threshold α ranging from 90% to 100%. The number of SVMs in the EOSVM classifier is $n = 100$. For each of the 12 connectivity measures, we execute EOSVM 20 times.

In Fig. 9, the red lines refer to the classification accuracy from the first group of connectivity measures (PSDD, PCC, COH, ICOH, PLV, and LI). The blue lines represent the classification accuracy from the second group of connectivity measures, which are incorporated with the recursive cosine function. It is observed from all six subfigures in Fig. 9 that the first five subfigures (Fig. 9(a) through Fig. 9(e)) demonstrate better performance from red lines than that from blue lines, indicating better accuracy performance from embedding the recursive cosine function into the corresponding connectivity measures. The levels of accuracy performance from both PLI and CPLI in the last subfigure

TABLE IV
CLASSIFICATION RESULTS FROM CPSDD

Voting threshold α	(Mean, SD) (%)			R_H (%)
	Accuracy	Sensitivity	Specificity	
1.00	100.00, 0.00	100.00, 0.00	100.00, 0.00	22.36
0.99	99.58, 1.86	100.00, 0.00	98.33, 7.45	28.47
0.98	99.16, 2.59	100.00, 0.00	97.75, 6.97	30.28
0.97	98.21, 3.20	100.00, 0.00	95.79, 7.55	35.14
0.96	95.81, 3.54	100.00, 0.00	89.29, 9.10	38.19
0.95	95.85, 3.15	100.00, 0.00	89.60, 7.95	41.25
0.94	95.47, 2.70	100.00, 0.00	88.69, 6.77	45.56
0.93	94.53, 1.93	100.00, 0.00	86.07, 4.90	45.69
0.92	94.55, 2.23	100.00, 0.00	86.25, 5.30	47.92
0.91	93.52, 1.84	100.00, 0.00	83.99, 3.91	49.03
0.90	93.98, 1.37	100.00, 0.00	84.52, 3.30	50.42

TABLE V
CLASSIFICATION RESULTS FROM CPLV

Voting threshold α	(Mean, SD) (%)			R_H (%)
	Accuracy	Sensitivity	Specificity	
1.00	99.17, 3.73	100.00, 0.00	98.33, 7.45	11.11
0.99	93.93, 10.09	98.75, 5.59	89.58, 16.86	14.72
0.98	87.18, 12.17	95.50, 9.30	79.67, 20.05	18.33
0.97	89.41, 10.16	94.58, 9.85	86.25, 20.64	20.14
0.96	78.85, 8.69	89.61, 10.16	70.00, 18.14	26.11
0.95	75.59, 6.48	89.81, 8.74	61.25, 9.54	29.44
0.94	75.82, 4.78	90.71, 7.10	59.74, 9.77	34.44
0.93	71.24, 5.36	85.78, 4.79	56.08, 9.18	37.50
0.92	72.66, 3.82	87.98, 1.92	54.02, 8.20	43.06
0.91	72.17, 4.77	88.24, 1.93	53.36, 6.73	44.44
0.90	72.96, 5.27	88.40, 1.72	54.67, 9.72	44.72

(Fig. 9(f)) are too low to be accepted regardless of whether or not the recursive cosine function is used. This excludes PLI and CPLI from the list of connectivity measures in our further experiments.

A further observation of Fig. 9 shows that in the remaining 10 connectivity measures after excluding PLI and CPLI, only CPSDD and CPLV give over a classification accuracy of over 90%, which is considered to be necessary for a clinically reliable diagnosis decision. Therefore, in our further experiments to be presented below, we concentrate on these two connectivity measures, i.e., CPSDD and CPLV.

3) *Brain Connectivity Measures CPSDD and CPLV:* Table IV tabulates the classification results of EOSVM with CPSDD. In addition to Fig. 9(a), this table adds more information about the performance of EOSVM classifications embedded with CPSDD, including Sensitivity, Specificity, and R_H under different settings of the majority voting threshold α ranging from 90% to 100%.

It is seen from Table IV that when the voting threshold α is between 0.97 to 1.00, all evaluation results from the first group of metrics (accuracy, sensitivity, and specificity) are higher than 95%. More specifically, when $\alpha = 0.97$, R_H reaches to its highest value 35.14%, implying that 35.14% of the subjects are diagnosed with high confidence.

Because the accuracy of EOSVM classifications with CPLV is shown in Fig. 9 to be higher than 90% in a small range of α , we also tabulated in Table V some additional information about the performance of EOSVM classifications with CPLV and α ranging from 90% to 100%. It is observed from Table V that only when α is set to 100%, will the three evaluation metrics,

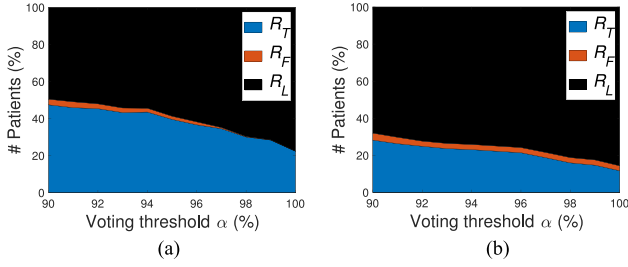


Fig. 10. EOSVM classifications with CPSDD and PSDD.

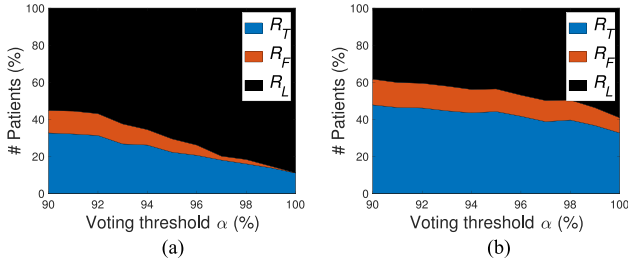


Fig. 11. EOSVM classifications with CPLV and PLV.

i.e., accuracy, sensitivity, and specificity be all greater than 90% (with $R_H = 11.11\%$).

4) Further Discussions on the Two Connectivity Measures:

The experimental results presented above show the effectiveness of EOSVM classifications with the two connectivity measures CPSDD and CPLV. It would be interesting to know how much percentage of patients with brain injuries can be diagnosed with DoC or wakefulness directly with high confidence by using the EOSVM classifier embedded with CPSDD and CPLV.

We evaluate the three performance metrics R_T , R_F and R_L , which are defined in Eqs. (16), (17), and (15), respectively. The voting threshold α is set in the range from 90% to 100%. For CPSDD and corresponding PSDD, the evaluation results are shown in Fig. 10. It is seen from Fig. 10(a) that with the increase of α , both R_T and R_F decrease, and meanwhile R_L keeps increasing. Our quantitative calculations reveal that when the voting threshold α is increased to 97%, the first group of three performance metrics, i.e., accuracy, sensitivity, and specificity, reach 98.21%, 100%, and 95.79%, respectively. These results have been presented in Table IV. In this situation, R_T reaches as high as 35.14% and meanwhile R_F becomes close to zero, meaning that about 35% of the patients could be diagnosed correctly. With Eq. (18), $R_H \rightarrow R_T$ when $R_F \rightarrow 0$.

For comparison, we also visualize in Fig. 10(b) the performance of EOSVM classifications with PSDD. In this figure, R_T is much smaller than that from CPSDD (Fig. 10(a)). In addition, R_F does not show improvement (i.e., a decrease) when the voting threshold α increases from 90% to 100%. Thus, our proposed CPSDD outperforms PSDD in both accuracy (Fig. 9(a)) and R_T (Fig. 10(a)) for the diagnosis of patients with brain injuries to DoC or wakefulness.

Fig. 11 visualizes the performance of EOSVM with CPLV and PLV in terms of R_T , R_F , and R_L for the voting threshold α ranging from 90% to 100%. It shows a similar pattern to Fig. 10, i.e., when α increases, R_T and R_F decrease while R_L rises.

For CPLV in Fig. 11(a), our quantitative calculations indicate that only when α increases to 100%, will all the three metrics accuracy, sensitivity, and specificity become higher than 90% for clinically reliable diagnose decision. The accuracy, sensitivity and specificity are 99.17%, 100%, and 98.33%, respectively. However, in this case, only about 11.11% of patients can be diagnosed correctly, i.e., $R_T = 11.1\%$. This R_T value of 11.11% from CPLV is much lower than the R_T value of 22.36% from our proposed CPSDD.

The classifications of EOSVM with PLV are depicted in Fig. 11(b). Comparisons between Fig. 11(b) and Fig. 11(a) reveal that R_F from using PLV is consistently higher than that from using CPLV in the full range of α though R_T is also higher. A higher R_T value implies a higher risk of classifying a subject incorrectly to either DoC or wakefulness and thus potentially more serious consequences, which medical practitioners always try to avoid. Thus, PLV is not as effective as CPLV in EOSVM classifications.

The design of EOSVM in this study contributes to the automated detection of DoC. As we focus on the classification of patients with brain injuries to either DoC or wakefulness, a test with high sensitivity is useful for ruling out disease [33]. Sensitivity in this study refers to the ability of the analysis to correctly detect patients with DoC who do have DoC (i.e., true positives). Tables IV and V show that the classification results have better sensitivity than specificity.

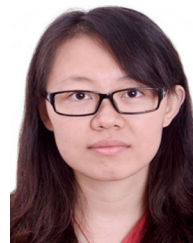
VII. CONCLUSION

In this paper, we have explored continuous detection of DoC in patients with brain injuries through EEG connectivity and machine learning. A connectivity measure PSDD has been proposed, which is further improved to CPSDD by incorporating a recursive cosine function. The recursive cosine function has also been used to improve other five connectivity measures, PCC, COH, ICOH, PLV, and PLI in the same way. Among the 12 connectivity measures, CPSDD and CPLV are shown to be two effective measures. Particularly, CPSDD has demonstrated the best classification performance from our EOSVM classifier. With a voting threshold of 97%, it is able to diagnose about 35% of patients with brain injury correctly. The accuracy, sensitivity, and specificity have reached 98.21%, 100% and 95.79%, respectively. The 35% of true classifications with high confidence also implies a 35% saving of the resources of manpower, time, and pathological tests, which would otherwise be consumed in traditional clinical checks.

REFERENCES

- [1] S. Suwatcharangkoon *et al.*, "Loss of consciousness at onset of subarachnoid hemorrhage as an important marker of early brain injury," *JAMA Neurol.*, vol. 73, no. 1, pp. 28–35, Jan. 2016.
- [2] J. T. Giacino *et al.*, "Practice guideline update recommendations summary: Disorders of consciousness," *Arch. Phys. Med. Rehabil.*, vol. 99, no. 9, pp. 1699–1709, Sep. 2018.
- [3] J. Whyte *et al.*, "Medical complications during inpatient rehabilitation among patients with traumatic disorders of consciousness," *Arch. Phys. Med. Rehabil.*, vol. 94, no. 10, pp. 1877–1883, Oct. 2013.
- [4] P. B. Forgacs, M. M. Conte, E. A. Fridman, H. U. Voss, J. D. Victor, and N. D. Schiff, "Preservation of electroencephalographic organization in patients with impaired consciousness and imaging-based evidence of command-following," *Ann. Neurol.*, vol. 76, no. 6, pp. 869–879, 2015.

- [5] J. Claassen *et al.*, "Bedside quantitative electroencephalography improves assessment of consciousness in comatose subarachnoid hemorrhage patients," *Ann. Neurol.*, vol. 80, no. 4, pp. 541–553, Aug. 2016.
- [6] S. Chennu *et al.*, "Brain networks predict metabolism, diagnosis and prognosis at the bedside in disorders of consciousness," *Brain*, vol. 140, no. 8, pp. 2120–2132, May 2017.
- [7] B. He *et al.*, "Electrophysiological brain connectivity: Theory and implementation," *IEEE Trans. Biomed. Eng.*, vol. 66, no. 7, pp. 2115–2137, Jul. 2019.
- [8] G. Niso *et al.*, "HERMES: Towards an integrated toolbox to characterize functional and effective brain connectivity," *Neuroinformatics*, vol. 11, no. 4, pp. 405–434, 2013.
- [9] J. Cai *et al.*, "Dynamic graph theoretical analysis of functional connectivity in Parkinson's disease: The importance of Fiedler value," *IEEE J. Biomed. Health Inform.*, vol. 23, no. 4, pp. 1720–1729, Jul. 2019.
- [10] A. Zhang, J. Fang, F. Liang, V. D. Calhoun, and Y. Wang, "Aberrant brain connectivity in schizophrenia detected via a fast Gaussian graphical model," *IEEE J. Biomed. Health Inform.*, vol. 23, no. 4, pp. 1479–1489, Jul. 2019.
- [11] S. Afshari and M. Jalili, "Directed functional networks in Alzheimer's disease: Disruption of global and local connectivity measures," *IEEE J. Biomed. Health Inform.*, vol. 21, no. 4, pp. 949–955, Jul. 2017.
- [12] S.-E. Moon, S. Jang, and J.-S. Lee, "Convolutional neural network approach for EEG-based emotion recognition using brain connectivity and its spatial information," in *Proc. IEEE Int. Conf. Acoust., Speech Signal Process.*, Calgary, AB, Canada, 15–20 Apr. 2018, pp. 2556–2560.
- [13] C. Gómez, C. J. Stam, R. Hornero, A. Fernández, and F. Maestú, "Disturbed beta band functional connectivity in patients with mild cognitive impairment: An MEG study," *IEEE Trans. Biomed. Eng.*, vol. 56, no. 6, pp. 1683–1690, Jun. 2009.
- [14] F. Li *et al.*, "Differentiation of schizophrenia by combining the spatial EEG brain network patterns of rest and task P300," *IEEE Trans. Neural Syst. Rehabil. Eng.*, vol. 27, no. 4, pp. 594–602, Apr. 2019.
- [15] C. J. Stam, G. Nolte, and A. Daffertshofer, "Phase lag index: Assessment of functional connectivity from multi channel EEG and meg with diminished bias from common sources," *Hum. Brain Mapping*, vol. 28, no. 11, pp. 1178–1193, Nov. 2007.
- [16] E. Mikulan *et al.*, "Intracranial high- γ connectivity distinguishes wakefulness from sleep," *Neuroimage*, vol. 169, pp. 265–277, Apr. 2018.
- [17] J. Carrier, S. Land, D. J. Buysse, D. J. Kupfer, and T. H. Monk, "The effects of age and gender on sleep EEG power spectral density in the middle years of life (ages 20–60 years old)," *Psychophysiology*, vol. 38, no. 2, pp. 232–242, Mar. 2001.
- [18] C. C. de Vos, S. M. van Maarseveen, P. J. Brouwers, and M. J. van Putten, "Continuous EEG monitoring during thrombolysis in acute hemispheric stroke patients using the brain symmetry index," *J. Clin. Neurophysiol.*, vol. 25, no. 2, pp. 77–82, Apr. 2008.
- [19] A. Naro, P. Bramanti, A. Leo, M. Russo, and R. S. Calabr, "Transcranial alternating current stimulation in patients with chronic disorder of consciousness: A possible way to cut the diagnostic Gordian knot?" *Brain Topogr.*, vol. 29, no. 4, pp. 623–644, Jul. 2016.
- [20] S. Chennu *et al.*, "Brain networks predict metabolism, diagnosis and prognosis at the bedside in disorders of consciousness," *Brain*, vol. 140, no. 8, pp. 2120–2132, Aug. 2017.
- [21] M. Cavinato *et al.*, "Coherence and consciousness: Study of fronto-parietal gamma synchrony in patients with disorders of consciousness," *Brain Topogr.*, vol. 28, no. 4, pp. 570–579, Jul. 2015.
- [22] S. Kashi, R. Feingold-Polak, B. Lerner, L. Rokach, and S. Levy-Tzedek, "A machine-learning model for automatic detection of movement compensations in stroke patients," *IEEE Trans. Emerg. Top. Comput.*, Apr. 2020, doi: [10.1109/TETC.2020.2988945](https://doi.org/10.1109/TETC.2020.2988945).
- [23] S. Supriya, S. Siuly, H. Wang, and Y. Zhang, "EEG sleep stages analysis and classification based on weighed complex network features," *IEEE Trans. Emerg. Top. Comput. Intell.*, Nov. 2018, doi: [10.1109/TETCI.2018.2876529](https://doi.org/10.1109/TETCI.2018.2876529).
- [24] A. Saha, A. Konar, and A. K. Nagar, "EEG analysis for cognitive failure detection in driving using Type-2 fuzzy classifiers," *IEEE Trans. Emerg. Top. Comput. Intell.*, vol. 1, no. 6, pp. 437–453, Dec. 2017.
- [25] A. Majid, S. Ali, M. Iqbal, and N. Kausar, "Prediction of human breast and colon cancers from imbalanced data using nearest neighbor and support vector machines," *Comput. Methods Programs Biomed.*, vol. 113, no. 3, pp. 792–808, 2014.
- [26] F. Wang, X. Zhang, F. Hu, F. Li, and Y.-C. Tian, "Quantitative electroencephalography analysis for improved assessment of consciousness in cerebral hemorrhage and ischemic stroke patients," *IEEE Access*, vol. 7, pp. 63 674–63 685, May 2019.
- [27] V. Sakkalis, "Review of advanced techniques for the estimation of brain connectivity measured with EEG/MEG," *Comput. Biol. Med.*, vol. 41, no. 12, pp. 1110–1117, Jul. 2011.
- [28] F. Wang, X. Zhang, F. Hu, F. Li, Y. Zhang, and Y.-C. Tian, "Using phase synchrony index for improved assessment of consciousness in ischemic stroke patients," *IEEE Access*, vol. 7, pp. 30 252–30 260, Mar. 2019.
- [29] J. A. Urigüen and B. Garcia-Zapirain, "EEG artifact removal state-of-the-art and guidelines," *J. Neural Eng.*, vol. 12, no. 3, p. 031001, Apr. 2015.
- [30] X. Chen, X. Xu, A. Liu, M. J. McKeown, and Z. J. Wang, "The use of multivariate EMD and CCA for denoising muscle artifacts from few-channel eeg recordings," *IEEE Trans. Instrum. Meas.*, vol. 67, no. 2, pp. 359–370, Nov. 2017.
- [31] Y. Soon, S. N. Koh, and C. K. Yeo, "Noisy speech enhancement using discrete cosine transform," *Speech Commun.*, vol. 24, no. 3, pp. 249–257, Jun. 1998.
- [32] J. Weston and C. Watkins, "Support vector machines for multi-class pattern recognition," in *Proc. Proc. - Eur. Symp. Artif. Neural Netw.*, Bruges, Belgium, 21–23 Apr. 1999, pp. 219–224.
- [33] D. G. Altman and J. M. Bland, "Diagnostic tests. 1: Sensitivity and specificity," *Brit. Med. J.*, vol. 308, no. 6943, p. 1552, Jun. 1994.



Fang Wang received the M.E. degree in 2013 from the Taiyuan University of Technology, Taiyuan, China, where she is currently working toward the Ph.D. degree. She is also a Visiting Ph.D. Student with Queensland University of Technology, Brisbane, QLD, Australia. Her research interests include EEG analysis, machine learning, and their applications in medical practice.



Yu-Chu Tian (Senior Member, IEEE) received the Ph.D. degree in computer and software engineering from the University of Sydney, Sydney, NSW, Australia, in 2009, and the Ph.D. degree in industrial automation from Zhejiang University, Hangzhou, China, in 1993. He is currently a Professor with the School of Computer Science, Queensland University of Technology, Brisbane, QLD, Australia. His research interests include big data computing, cloud computing, computer networks, optimization, artificial intelligence and machine learning, and control systems.



Xueying Zhang (Member, IEEE) received the Ph.D. degree in underwater acoustic engineering from Harbin Engineering University, Harbin, China, in 1998. She is currently a Professor with the College of Information and Computer, Taiyuan University of Technology, Taiyuan, China. Her research interests include auditory modeling, emotional speech recognition, EEG analysis, and machine learning.



Fengyun Hu received the MBBS degree in clinical medicine from Shanxi Medical College, Taiyuan, China, in 1983. She is currently a Chief Physician with the Shanxi Provincial Peoples Hospital affiliated with Shanxi Medical University, Taiyuan, China. Her research interests include cerebrovascular disease, epilepsy, and neurosis.